Third-order nonlinear optical properties of bismuth-borate glasses measured by conventional and thermally managed eclipse *Z* scan

A. S. L. Gomes,[a] E. L. Falcão Filho, and Cid B. de Araújo
Departamento de Física, Universidade Federal de Pernambuco, Cidade Universitária, Recife 50670-901, Brazil

Diego Rativa and R. E. de Araujo
Departamento de Eletrônica e Sistemas, Universidade Federal de Pernambuco, Recife, Pernambuco 50670-901, Brazil

Koichi Sakaguchi
Technical Research Laboratory, Nippon Sheet Glass Co., Ltd., Itami, Hyogo 664-8520, Japan

Francesco P. Mezzapesa, Isabel C. S. Carvalho,[b] and Peter G. Kazansky
Optoelectronics Research Centre, University of Southampton, Southampton SO17 1 BJ, United Kingdom

(Received 31 August 2006; accepted 5 December 2006; published online 8 February 2007)

Third-order nonlinearity one order of magnitude larger than silica is measured in bismuth-borate glasses presenting a fast response (<200 fs). The results for the sign and magnitude of the nonlinearity were obtained using a combination of the eclipse *Z* scan with thermal nonlinearity managed *Z* scan, whereas the Kerr shutter technique was employed to obtain the electronic time response of the nonlinearity, all performed with 76 MHz repetition rate 150 fs pulses at 800 nm. Conventional *Z* scans in the picosecond regime at 532 and 1064 nm were also independently performed, yielding the values of the third-order nonlinear susceptibilities at those wavelengths. The results obtained for the femtosecond response, enhanced third-order nonlinearity of this glass (with respect to silica), place this glass system as an important tool in the development of photonics devices. Electro-optical modulators, optical switches, and frequency converters are some of the applications using second-order nonlinear properties of the Bi-glass based on the rectification model. © *2007 American Institute of Physics*. [DOI: 10.1063/1.2434940]

I. INTRODUCTION

The search for applicable photonic materials, particularly glasses with high third-order nonlinear optical susceptibility $\chi^{(3)}$ has provided important advances in this field. In the recent years, host glasses with modified matrix network have been developed which led to improved third-order nonlinearities.[1–3] Applications of such glasses include all-optical switching,[4] optical limiting,[5] and enhanced second-order nonlinearities.[6] In order to fully characterize such glasses, besides the linear properties, nonlinear characterization is required. Nowadays, two complementary techniques have been employed for such task: the *Z* scan[7] and some of its varieties,[8,9] for the sign and magnitude of the nonlinearity, and the Kerr shutter method,[10] which allows direct measurement of the electronic time response as well as the magnitude of the nonlinearity. Unlike the *Z*-scan method, from the Kerr shutter method one does not infer the sign of the nonlinearity nor the imaginary part (nonlinear absorption) of $\chi^{(3)}$. Therefore, both techniques are complementary.

In this article, we describe the characterization of the third-order nonlinear optical susceptibility of a family of highly nonlinear glasses based on bismuth borate (Bi_2O_3–ZnO–B_2O_3), whose second-order nonlinear optical susceptibility induced by thermal poling has been recently studied.[6] The results obtained for the fast response enhanced third-order nonlinearity of this glass, with respect to silica glasses, corroborate the model proposed in Ref. 6 to explain the enhancement of its second order nonlinear optical susceptibility induced by thermal poling with the increase of the bismuth content.

The paper is organized as follows. In Sec. II, we describe the experimental procedures used. In Sec. III, we describe the experimental results of the measured third-order nonlinearity, both in magnitude, sign, and response time of their real and imaginary parts. The measurements have been performed at three different wavelengths and different time regimes, namely, 532 nm, 1064 nm in the picosecond regime, and 800 nm in the femtosecond regime. In Sec. IV we discuss the results, compare the values obtained with some well known nonlinear optical materials, and draw the main conclusions of this work.

II. EXPERIMENTAL PROCEDURES

A. Glass samples

The fabrication of the glass samples was performed by melting and quenching in the ternary Bi_2O_3–ZnO–B_2O_3 system.[6] For each glass, batch of 400 g glass was obtained by thoroughly mixing adequately weighed reagent grades of Bi_2O_3, ZnO, and B_2O_3. The batch was put in a platinum

[a]Electronic mail: anderson@df.ufpe.br
[b]Permanent address: Pontifícia Universidade Católica do Rio de Janeiro, Departamento de Física, 22453-900 Rio de Janeiro, Brazil.

crucible and melted in an electric furnace at 1000 °C in air for 1.5 h. During melting, the glass melt was stirred thoroughly several times to improve its homogeneity. After the melting, the glass melt was poured onto a stainless-steel plate and put in an electric furnace. The glass was annealed at its glass-transition temperature for 30 min and subsequently cooled to room temperature in the furnace. Boron and zinc ions acted as network formers and modifiers, respectively. At low Bi_2O_3 content, bismuth ions acted as network formers. As the Bi_2O_3 content increased, the glass-transition temperature (T_g) decreased while the glass density (ρ) and the refractive index (n) increased. Water was present in the glass matrix in the form of OH bonds (OH impurity level was in the range of a few hundreds ppm and varied from batch to batch). Optical transmission spectra exhibited a flat maximum between ~500 and ~2000 nm and an UV absorption edge which shifted towards wavelengths longer than 400 nm (but shorter than 500 nm) with increased Bi_2O_3. The glass family was named BZH,[6] and the samples studied in this work correspond to samples BZH2 ($25.0Bi_2O_3-37.5ZnO-37.5B_2O_3$) and BZH7 ($12.5.0Bi_2O_3-43.5ZnO-43.5B_2O_3$).[6]

B. *Z*-scan measurements

The well established *Z*-scan method[7] exploits the light-matter interaction so that an incident beam propagating inside a nonlinear medium induces a self-change in the phase that gives rise to a wave front distortion of the beam. In the original *Z*-scan setup (hereafter denominated conventional *Z* scan), by measuring the variation of the transmitted beam intensity through a small circular aperture placed in front of a detector in the far-field region, one can determine the sign and magnitude of the nonlinear refractive index $n_2 \propto \mathrm{Re}[\chi^{(3)}]$, while when the entire light beam passing through the sample is detected, the nonlinear absorption $\alpha_2 \propto \mathrm{Im}[\chi^{(3)}]$ is obtained. An important variation of the original setup, known as eclipse *Z* scan[8] employs a disk in front of the detector (instead of an aperture), such as the eclipsed beam collected by a lens is directed towards the detector. It has been shown[8] that this arrangement can provide up to two orders of magnitude higher sensitivity than the original *Z*-scan setup.

As the third-order nonlinear optical susceptibility can arise from different physical mechanisms, it is important to differentiate among them. For instance, thermal nonlinearities are almost always present in liquids and many glassy materials when excited with cw or quasi-cw (high repetition rate, several megahertzs) light sources. Generally, to avoid the manifestation of such thermal nonlinearities, low repetition rate single beams are used in the experimental methods, but with high peak power and other inherent experimental challenges, such as pulse to pulse fluctuations. However, very recently,[9] Gnoli *et al.* introduced a clever variation of the conventional *Z*-scan method which allows us to differentiate between the thermal nonlinearity and electronic nonlinearity, even using relatively low peak power and high repetition rate pulse trains.

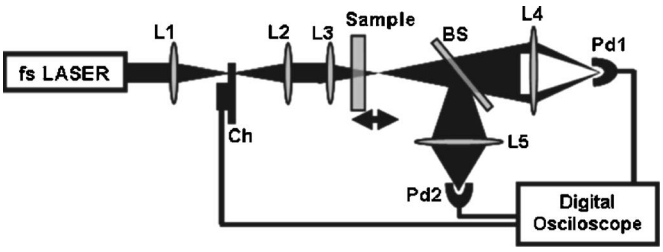

FIG. 1. Experimental setup for thermally managed eclipse *Z* scan.

To have a comprehensive characterization of the nonlinearity in the studied glasses, we employed the conventional *Z*-scan setup at two different wavelengths (532 and 1064 nm) using a pulsed picosecond laser, and at a third wavelength, 800 nm, using a combination of eclipse *Z* scan with thermal management, using a high repetition rate cw mode-locked laser.[11] In this way, a more sensitive arrangement with a very good signal to noise ratio was obtained.

The conventional *Z*-scan measurements were independently performed using a Q-switched and mode-locked Nd:YAG (yttrium aluminum garnet) laser delivering pulses of 100 ps at 1064 nm or 80 ps at 532 nm full width at half maximum, as the light source. The experimental setup is similar to that shown in Fig. 1, except that the laser is the one described above, lenses L1, L2, and L3 are replaced by a single lens (10 cm focal distance lens focused the laser beam, so that the measured beam waist was ~20 μm) and a small aperture replaced the disk. In either case (1064 or 532 nm), a single pulse at a repetition rate of 10 Hz was selected using a pulse picker to avoid cumulative thermal effects. The samples (different thicknesses, around 1 mm) were mounted in a support placed in a computer-controlled translation stage that could be moved along the focus region in order to allow direct measurements of the nonlinear properties. A photodetector with an adjustable aperture in front of it was placed in the far-field region. The aperture size r_a is related to S, the linear aperture transmittance by $S=[1-\exp(-2r_a^2/w_a^2)]$, with w_a denoting the beam radius at the aperture for very low incident power.[7] A small aperture *Z*-scan experiment corresponds to $S \ll 1$, which is employed for n_2 measurements, and a wide or absent aperture means $S=1$, necessary for the determination of α_2. The z ordinate is measured along the beam propagation direction, and $z<0$ corresponds to locations of the sample between the focusing lens and its focal plane. A boxcar integrator was used in connection with a computer to record the signal.

The experimental setup employing the eclipse *Z* scan and thermal management is shown in Fig. 1. A Ti-saphire laser delivering pulses at 76 MHz, with 150 fs pulse duration, and 700 mW average power at 800 nm was used as the light source. A disk with 1.7 cm diameter was placed prior to a 10 cm focal distance lens (L4), in order to direct the eclipsed beam to the detector. The chopper is the new element responsible for the thermal management experimentally, introduced to modify the conventional *Z*-scan setup, as described in detail in Ref. 9. In short, the thermal management method consists in acquiring the time evolution of the *Z*-scan signal, for the sample placed in the prefocal and post-

focal positions of its focal plane with respect to lens L3. The time resolution of the system is determined by the chopper opening time, which depends on the finite size of the beam waist on the chopper wheel, and was 18 μs in our experimental setup. By delaying the photodetector (submicrosecond risetime) signal acquisition time with respect to the time zero (determined by the opening time of the chopper), the time evolution of the *Z*-scan signal at both the pre- and postfocal positions are obtained. The photodetector information is sent to a digital scope and then processed. From these measurements, and using the formalism described in Ref. 9, the *Z*-scan curves can be constructed and the contribution of the thermal and electronic nonlinearities can be inferred, provided no other mechanism besides the electronic nonlinearity are present in the relatively short time (several microseconds) of the chopper opening risetime. It is important to mention that, conversely to the conventional *Z* scan, in the eclipse *Z* scan a prefocal peak and a postfocal valley reveals a self-focusing Kerr nonlinearity, while a valley arising before a peak is representative of a self-defocusing Kerr nonlinearity. Also, in this case, the linear obstacle transmission is given by $S_e=[1-\exp(-2r_e^2/w_e^2)]$, with r_e being the obstacle radius and w_e the beam radius (the subscript e denotes eclipse). In the present experiment we have $S=0.99$.

As will be shown later, a rise or decay time and crossing of the two temporal evolution curves (pre- and postfocal distances) indicates the presence of both electronic and thermal nonlinearities, and that the signs of both nonlinear indices are opposite. When a rise or decay time appears without crossing, the signs of the thermal and electronic nonlinearities are the same. A flat temporal evolution indicates the absence of thermal nonlinearity.

C. Kerr shutter measurements

Kerr shutter measurements were performed in the femtosecond regime, since the main aim was to determine the time response of the electronic nonlinearity. The Kerr shutter setup is well known[10] and we employed the beam delivering pulses with 150 fs duration at 76 MHz repetition rate from a Ti:sapphire laser operating at 800 nm, which was split into two beams with different intensities (10×1 intensity ratio), as the light source. The electric field of the strong (pump) beam was set at 45° with respect to the electric field of the weak (probe) input beam. When the pulses of the two beams overlap spatially and temporally at the sample position, the probe beam polarization rotates due to the birefringence induced in the sample by the pump beam. Then, a fraction of the probe beam passes through a polarizer crossed to the input probe beam polarization. A slow detector was used to record the probe signal as a function of the time delay between pump and probe beams.

III. EXPERIMENTAL RESULTS

For all the measurements (Kerr shutter and *Z* scan) CS_2 was used as a standard material to confirm our data. For the thermally managed eclipse *Z* scan, we also employed fused silica as a material for comparison, since in this case the system was sensitive enough to measure the silica nonlinearity, which is two orders of magnitude smaller than for CS_2, even at the low peak power employed.

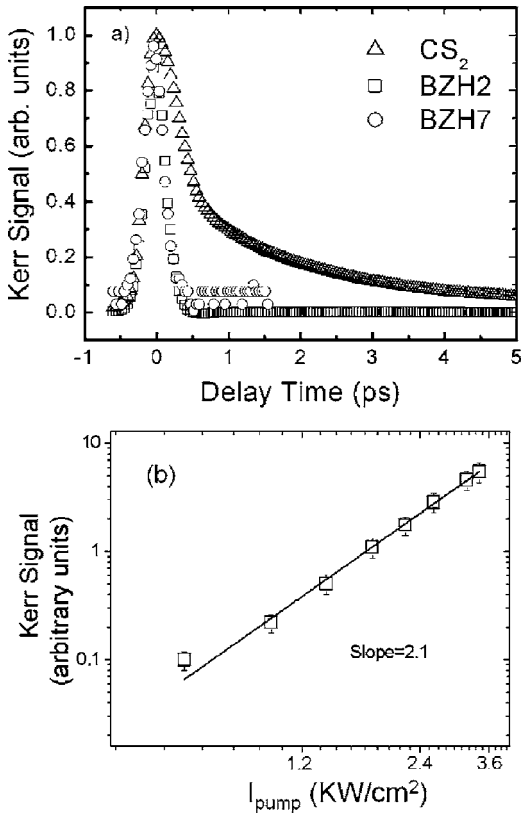

FIG. 2. (a) Normalized Kerr shutter signal for CS_2 (2 mm), glasses BZH2 and BZH7 (1 mm), obtained at the same pump intensity. (b) Signal intensity vs pump power for the Kerr shutter measurement of glass BZH2.

Let us start by describing the temporal measurements obtained with the Kerr shutter. Figure 2 shows the results obtained for CS_2 and the two glass samples. As is well known, CS_2 has two decay times, a fast one (<50 fs) and a slower one (~2 ps), which can also be used to verify the system response, as seen in Fig. 2(a). From that figure, the measured fast decay in the glass samples is actually limited by the pulse duration (150 fs), whereas the slower one is about 2 ps in CS_2, as expected, and due to a reorientational nonlinearity.[10] Also shown in Fig. 2(b) is the power dependence of the Kerr signal intensity versus pump power. A slope of 2 curve is observed, indicating a dependence of the signal transmitted intensity with the square of pump beam intensity ($I_{\text{tran}} \propto I_{\text{probe}} I_{\text{pump}}^2$), which has been explained before[10] and arises due to the small phase shift imposed by the relatively low intensity employed.

Figures 3 and 4 show the results of the conventional *Z*-scan experiment using the pulsed Nd:YAG source at its fundamental and second harmonic optical frequencies. Each data point in Figs. 3 and 4 represents the average of 20 shots and four scans. The solid lines are the best-fit curves obtained using the procedure of Ref. 7.

For the sake of comparison as well as direct intensity measurement, shown in Fig. 3(a) is the result for the nonlinear refractive index of CS_2, from which one infers the beam intensity (considering the literature value of n_2 for CS_2 at

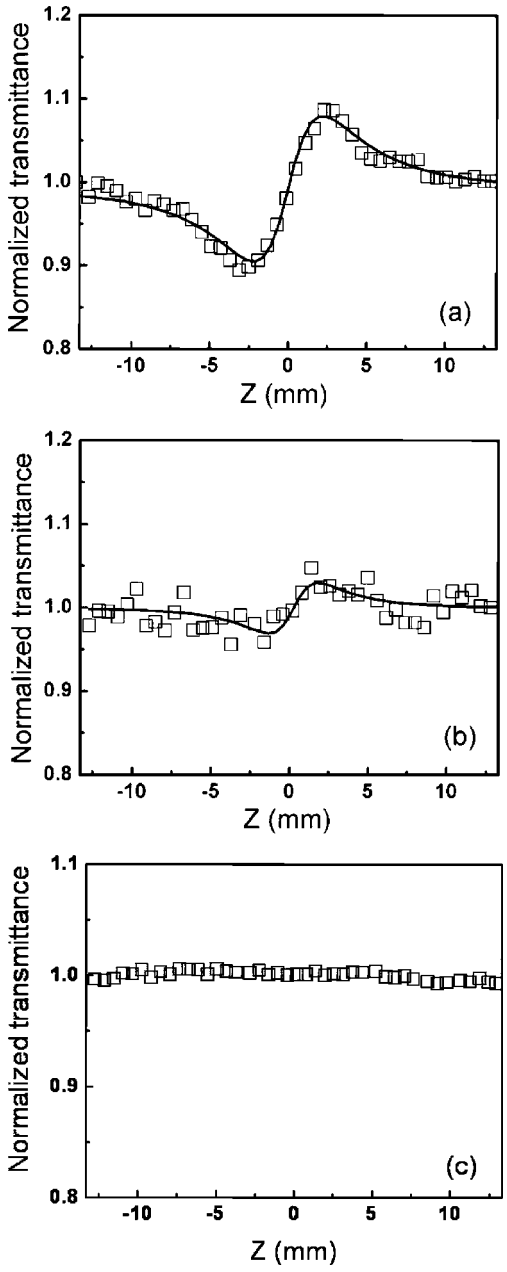

FIG. 3. Measured nonlinear refraction ($S \ll 1$) at 1064 nm for (a) CS2 and (b) BZH2. Measured nonlinear absorption ($S=1$) for BZH2 (c).

1064 nm to be $n_2 \cong 3.3\times10^{-14}$ cm^2/W) to be 1.2 GW/cm^2. Figure 3(b) shows the result for the glass sample BHZ2. The total change in the normalized transmittance, for $S<1$, is given by $\Delta T=0.406\ kL_{eff}n_2I_{pump}$, where I_{pump} is the excitation peak intensity, $k=2\pi/\lambda$, $L_{eff}=[1-\exp(-\alpha_0 L)]/\alpha_0$, L is the sample length, and λ is the excitation light wavelength. Thus, for the same intensity at 1064 nm, one infers the value of $n_2 \cong 1.0\times10^{-14}$ cm^2/W for this glass, and the sign of the nonlinearity is the same as for CS_2, denoting a focusing media ($n_2>0$). Similar to CS_2, the BZH2 sample presents a negligible nonlinear absorption coefficient, or at least limited by our experimental sensitivity (<0.02 cm/GW). Figure 3(c) shows the obtained result, using the full aperture, for the sake of completeness. For the BZH7 sample, the value of n_2 at 1064 nm was below our experimental sensitivity (although an estimative value is given in Sec. IV) and α_2 is expected to be negligible at this wavelength.

The same set of measurements was performed at 532 nm, as shown in Fig. 4. Figure 4(a) shows the CS_2 result at 532 nm (from which the intensity value of 1.3 GW/cm^2 was inferred), using the value of the nonlinearity for CS_2 at 532 nm to be $n_2 \cong 3.1\times10^{-14}$ cm^2/W.[12] As expected and known, the sign of n_2 for CS_2 at 532 nm, Fig. 4(a), is the same as for 1064 nm, since the material is transparent and there is no physical or chemical difference in this wavelength interval. As for the two evaluated glasses, Figs. 4(b) and 4(c), the sign is the same and the inferred magnitude of the nonlinearity is n_2 (BHZ2)$=3.0\times10^{-14}$ cm^2/W and n_2 (BHZ7)$=1.8\times10^{-14}$ cm^2/W.

As for the nonlinear absorption coefficient, Figs. 4(d) and 4(e), it can be seen that there is a sizable nonlinear absorption, differently from CS_2 and from the 1064 nm measurement. The inferred values of the absorptive nonlinearities are α_2 (BHZ2)=5.5 cm/GW and α_2 (BHZ7)=1.5 cm/GW. In this case, for the open aperture scheme ($S=1$), the nonlinear absorption coefficient is related with the total change in the normalized transmittance by $\Delta T=(2)^{-3/2}L_{eff}\alpha_2 I_0$.

The results of the thermally managed eclipse Z-scan measurements performed at 800 nm for CS_2 (2 mm thick cuvette) and SiO_2 (1.6 mm sample) are similar to those shown in Ref. 9, except the curves are inverted with respect to pre- and postfocal positions, as explained before. The obtained values for the nonlinearities are shown in Table I. Figures 5(a)–5(d) shows the thermally managed eclipse Z-scan results obtained for the glasses BZH7 [Figs. 5(a) and 5(b)] and BZH2 [Figs. 5(c) and 5(d)]. Notice that a small thermal component is seen for the BZH2 glass, which does not appear for the BZH7 sample. From these measurements, the values of $n_{2,electronic}$ (BHZ2)$=2.9\pm0.1\times10^{-15}$ cm^2/W extrapolated for $t=0$ and $n_{2,thermal}$ (BHZ2)$=3.1\pm0.1\times10^{-15}$ cm^2/W at $t=800$ μs were inferred for electronic and thermal nonlinearity, respectively, being both of positive sign (focusing nonlinearity, since the eclipse Z-scan inverts the signature). As for BZH7 glass, no thermal nonlinearity was observed and a positive $n_{2,electronic}$ (BHZ7)$=1.3\pm0.3\times10^{-15}$ cm^2/W was measured. At this temporal and spectral regimes, no nonlinear absorption was experimentally detected for the maximum peak powers available in our experiment, even though the excitation wavelength was close to the absorption edge for two-photon absorption.

IV. DISCUSSION AND CONCLUSIONS

Table I summarizes the values for the electronic nonlinearities of the measured materials, indicating the pulse duration and wavelengths. The values for the CS_2 and SiO_2 were obtained from the literature, and used as standard materials, and the measured values for the two glasses studied are also shown. First, one should notice that only at 532 nm a nonlinear absorption coefficient is measured, which is in good agreement with the fact that the glass linear absorption spectrum shows a strong absorption below 400 nm, thus being susceptible to nonlinear (two photon) absorption below

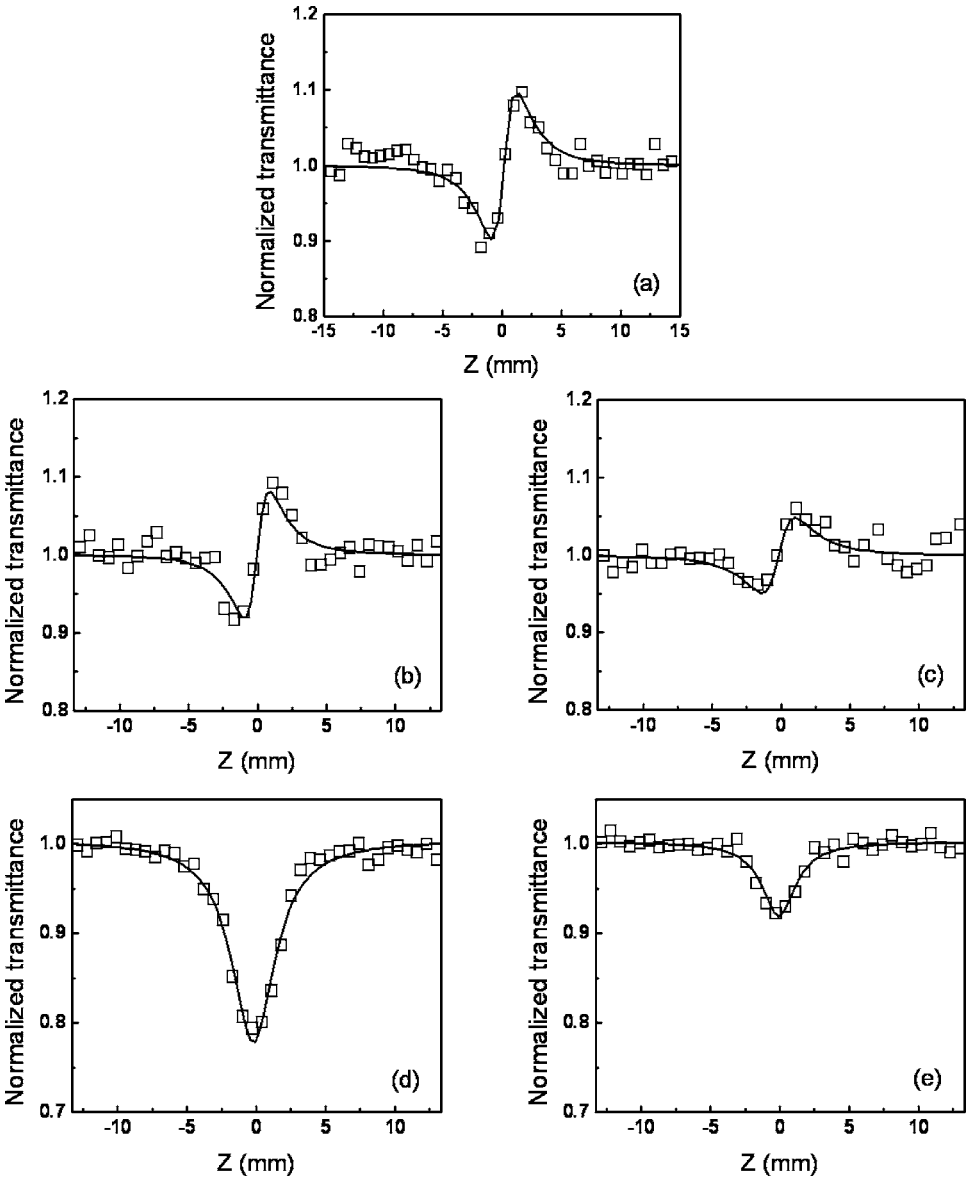

FIG. 4. Measured nonlinear refraction ($S \ll 1$) at 532 nm for (a) CS2, (b) BZH2, and (c) BZH7. Measured nonlinear absorption ($S=1$) at 532 nm for (d) BZH2 and (e) BZH7. For all data $I=1.3$ GW/cm^2.

TABLE I. Measured values of n_2 (at $t=0$, extrapolated using the formalism of Ref. 9) and α_2 for bismuth borate glasses. CS_2 and SiO_2 values from the literature in similar spectral and temporal excitation conditions are also shown.

	$\lambda=1064$ nm, $\tau_p=100$ ps		$\lambda=532$ nm, $\tau_p=80$ ps		$\lambda=800$ nm, $\tau_p=150$ fs	
	n_2 (cm^2/W)	α_2 (cm/GW)	n_2 (cm^2/W)	α_2 (cm/GW)	n_2 (cm^2/W)	α_2 (cm/GW)
CS_2	3.3×10^{-14}[a]	<0.02	3.1×10^{-14}[a]	0.09[b]	$(2.5\pm0.7)\times10^{-15}$	1.2×10^{-4}[c]
BZH7	$<5\times10^{-15}$	<0.02	$(1.8\pm0.4)\times10^{-14}$	1.5 ± 0.2	$(1.3\pm0.3)\times10^{-15}$	<0.01
BZH2	$(1.0\pm0.2)\times10^{-14}$	<0.02	$(3.0\pm0.2)\times10^{-14}$	5.5 ± 0.2	$(2.9\pm0.2)\times10^{-15}$	<0.01
SiO_2	3.2×10^{-16}[d]	<0.02	2.2×10^{-16}[d]	<0.02	2.2×10^{-16}[e]	<0.01

[a]Reference 7.
[b]Reference 16.
[c]Reference 9.
[d]Reference 15.
[e]Reference 13.

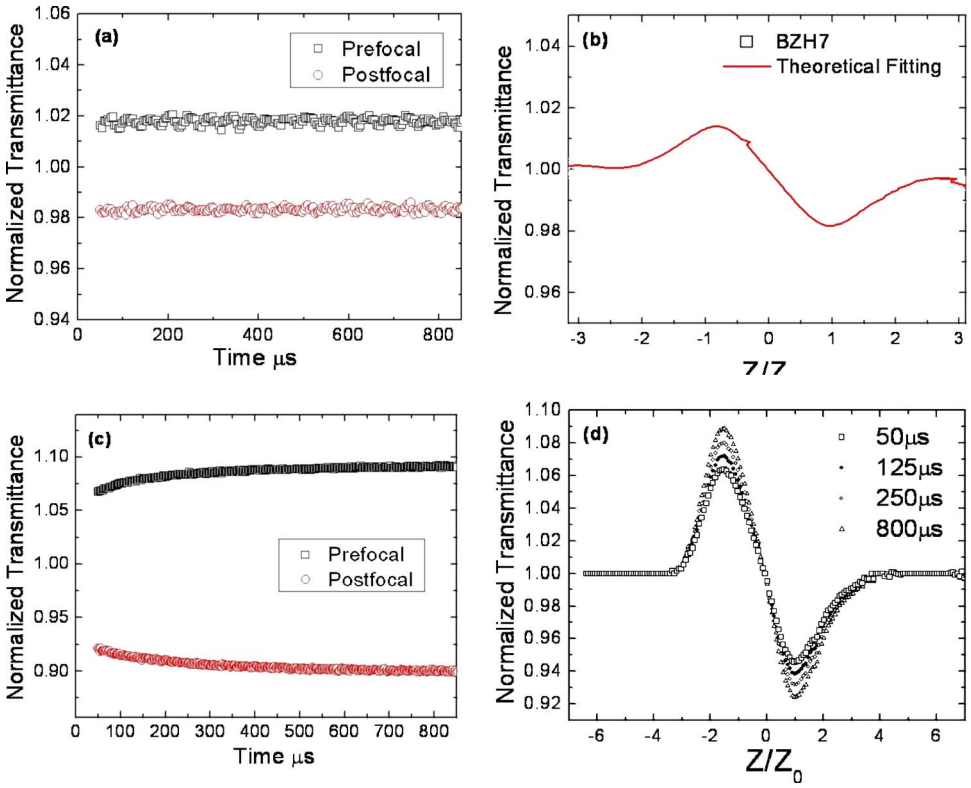

FIG. 5. Thermally managed eclipse *Z*-scan measurements. (a) Time evolution and (b) *Z*-scan signature for glass BZH7; (c) time evolution and (d) z-scan signature for glass BZH2. The curve at $t=0$ is extrapolated using the formalism of Ref. 9.

800 nm excitation wavelength, which is evidenced when using 532 nm excitation wavelength. Nonlinear absorption can be exploited for optical limiting application, and we have shown in a separate publication that this glass is very suitable for such application, particularly in the nanosecond regime.[14]

For the visible and near-infrared excitation wavelengths studied, the electronic nonlinearity is positive for all the materials, characteristic of self-focusing nonlinearity. In the picosecond regime, the measured nonlinear refractive index is higher for the BZH2 glass than for the BZH7 for both wavelengths. At 1064 nm, the value of n_2 for the BZH7 glass is below the sensitivity of our setup, and the data were within the noise floor. A conservative estimative, based on the BZH2 value and also on the value measured at 800 nm (although in the femtosecond regime) is shown in Table I. For the BZH2, as seen in Fig. 3(b), the signal is barely above the noise floor, and with the theoretical fit, its value can be inferred. At 532 nm, the values of n_2 and α_2 for both glasses are clearly obtained, and the higher values of n_2 are strong evidence of the contribution of two-photon absorption at this wavelength. The contribution of the two-photon absorption is also confirmed by the peak-to-valley distance in the transmittance curves for nonlinear refraction (see Figs. 3 and 4), which is shorter at 532 nm than at 1064 nm, approaching the theoretical values of $1.13z_0$ for the 532 nm curve and $1.7z_0$ for the 1064 nm curve.[7]

At 1064 nm, in the picosecond regime, the value of n_2 (BZH2) $\sim 31n_2$ (SiO_2). This result corroborates the assumption made in Ref. 6, based on Miller's rule,[12] that the third-order nonlinear optical susceptibility of glass BZH2 would be 33.3 times higher than for SiO_2, thus explaining the use of the rectification model for the second-order optical nonlinearity enhancement in such glass (and for the whole family of bismuth-borate glasses). The second harmonic generation measurements in Ref. 6 were performed in this picosecond regime, and the enhancement of the nonlinearity arose due to the incorporation of Bi_2O_3 in the pristine glass. The value of the linear refractive index of glass BZH2 is 1.91,[6] as compared to silica, whose refractive index is 1.45.

At 800 nm in the femtosecond regime, since we employed a much more sensitive method, the thermally managed eclipse *Z* scan, we could obtain the values of n_2 for both glasses as well as for silica. From the data in Table I, we infer that n_2 (BZH7) $\sim 6n_2$ (SiO_2) and n_2 (BZH2) $\sim 13n_2$ (SiO_2). The enhancement factor of the real part of the third-order optical nonlinearity is thus about two times higher for the BZH2 glass than for BZH7 glass, compared to SiO_2. This is again in agreement with Miller's rule, since the enhancement factor for the BZH7 should be about $\frac{1}{2}$ of that of BZH2 compared to SiO_2, since the refractive index of BZH7 is 1.79. Notice that the thermal contribution to the nonlinearity does not change sign, with respect to the electronic one (as is the case for CS_2), being both positive.

In summary, we have characterized the third-order nonlinear optical susceptibility of two glasses recently prepared aiming at enhancing their second-order nonlinear optical susceptibility. By modifying the glass network such as to increase the linear refractive index, an increase in the third-order optical nonlinearity was expected. Through the rectification model, this would explain the observed efficiently generated second harmonic in the poled sample, compared to silica glass.[6] The measurement performed here exploited the conventional *Z*-scan method, as well as a variation of the *Z* scan, namely, the thermally managed

eclipse Z scan.[11] The values for the electronic n_2 were obtained, as well as the thermal contribution, and the results are in very good agreement with the work of Ref. 6. The glasses used can also be exploited for other photonic applications, since they have nonlinearities among the highest reported in the literature,[1,17] have already been pulled in fiber form and demonstrated as broadband optical amplifier.[18] Another important application has been recently developed, as an optical limiting device, as exploited in Ref. 14.

ACKNOWLEDGMENTS

The authors from Universidade federal de Pernambuco wish to thank CNPq, CAPES, and FACEPE, Brazilian Agencies, for financial support. They are also part of the Institute of Millenium in Nonlinear Optics, Photonics and Biophotonics, supported by CNPq, to whom the support is also acknowledged. All the authors are very grateful to Nippon Sheet Glass Co. Ltd. (NSG) in Japan for providing the samples. One of the authors (I.C.S.C.) acknowledges NSG for funding her Research Fellowship at the Optoelectronics Research Centre.

[1] N. Sugimoto, H. Kanbara, S. Fujiwara, K. Tanaka, Y. Shimizugawa, and K. Hirao, J. Opt. Soc. Am. B **16**, 1904 (1999); T. Hasegawa, T. Nagashima, and N. Sugimoto, Opt. Commun. **250**, 411 (2005).
[2] S. Smolorz, I. Kang, F. Wise, B. G. Aitken, and N. F. Borelli, J. Non-Cryst. Solids **256**, 310 (1999).
[3] A. J. Ikushima, T. Fujiwara, and K. Saito, J. Appl. Phys. **88**, 1201 (2000).
[4] J. M. Harbold, F. Ö. Ilday, F. W. Wise, J. S. Sanghera, V. Q. Nguyen, L. B. Shaw, and I. D. Aggarwal, Opt. Lett. **27**, 119 (2002).
[5] I. Kang, T. D. Krauss, F. W. Wise, B. G. Aitken, and N. F. Borrelli, J. Opt. Soc. Am. B **12**, 2053 (1995).
[6] O. Deparis, F. P. Mezzapesa, C. Corbari, P. G. Kazansky, and K. Sakaguchi, J. Non-Cryst. Solids **351**, 2166 (2005).
[7] M. Sheik-Bahae, A. A. Said, T. H. Wei, D. J. Hagan, and E. W. Van Stryland, IEEE J. Quantum Electron. **QE-26**, 760 (1990).
[8] T. Xia, D. J. Hagan, M. Sheik-Bahae, and E. W. Van Stryland, Opt. Lett. **19**, 317 (1994).
[9] A. Gnoli, L. Razzari, and M. Righini, Opt. Express **13**, 7976 (2005).
[10] *Semiconductors Processes Probed by Ultrafast Laser Spectroscopy*, edited by R. R. Alfano (Academic, New York, 1984), Vol. 1, p. 409.
[11] A. S. L. Gomes, E. L. Falcão Filho, C. B. de Araújo, D. Rativa, and R. E. de Araujo, Proceedings of SPIE, Photonics West 2007, paper PN6455-36.
[12] G. I. Stegeman, in *Nonlinear Optics of Organic Molecules and Polymers*, edited by H. S. Nalva and S. Miyata (CRC, Boca Raton, FL, 1997), p. 799.
[13] A. J. Taylor, G. Rodriguez, and T. S. Clement, Opt. Lett. **21**, 1812 (1996).
[14] T. R. Oliveira, L. de S. Menezes, A. S. L. Gomes, C. B. de Araújo, K. Sakaguchi, F. P. Mezzapesa, I. C. S. Carvalho, and P. G. Kazansky, Appl. Phys. Lett. **89**, 211912 (2006).
[15] R. DeSalvo, A. A. Said, D. J. Hagan, E. W. Van Stryland, and M. Sheik-Bahae, IEEE J. Quantum Electron. **32**, 1324 (1996).
[16] X. Liu, S. Guo, H. Wang, N. Ming, and L. Hou, J. Nonlinear Opt. Phys. Mater. **10**, 431 (2001).
[17] H. Nasu, T. Ito, H. Hase, J. Matsuoka, and K. Kamiya, J. Non-Cryst. Solids **204**, 78 (1996).
[18] Y. Kondo, M. Ono, K. Kageyama, M. Reys, and N. Sugimoto, Electron. Lett. **41**(6) (2005).